

BASICITY AND NUCLEOPHILICITY EFFECT IN CHARGE TRANSFER
OF AlH_3 -BASE ADDUCTS: THEORETICAL APPROACHMohammed Aichi^{1, 2}, Meriem Hafied^{2, 3, ✉}<https://doi.org/10.23939/chcht17.02.221>

Abstract. This study permits to explore the interactions involved in Lewis acid (AlH_3) and Lewis bases: CO ; H_2O ; NH_3 ; PH_3 ; PCl_3 ; H_2S ; CN^- ; OH^- ; O_2^{2-} ; F^- ; $\text{N}(\text{CH}_3)_3$; N_2 ; N_2H_4 ; N_2H_2 ; $\text{C}_5\text{H}_5\text{N}$; $\text{C}_6\text{H}_5\text{-NH}_2$. By means of DFT theory calculations with B3LYP functional using 6-31G(d,p) basis set and in order to check the effects of both the donor and the acceptor in the establishment of the different adducts we focused mainly on the calculation of the energetic gap $\Delta E_{\text{HOMO-LUMO}}$, Gibbs energies ΔG , the angle (θ) in AlH_3 -base and the interaction energy values E_{inter} . The several parameters of the reactivity (electrophilicity index (ω), nucleophilicity (N), chemical potential (μ), hardness (η), and polarizability (α)) are also calculated to define the weak interaction as well as to distinguish between the nucleophilicity and basicity of different Lewis bases. The results showed that the electronic charge transfer is estimated to be important in the systems where the interaction is established between Al and anionic bases, and the electron donor power is predictable for O^{2-} , F^- , OH^- , and CN^- . The pseudo-tetrahedral adduct arrangements depend on the parameter geometries (bond length interaction and θ angle) and Gibbs energies ΔG characterizing the main stability.

Keywords: Lewis acid-base interaction, stability, DFT, NBO analysis.

1. Introduction

Lewis acid-base interaction adducts include a partially formed dative bond that provides several new and intriguing viewpoints on molecular structure and bonding.¹ The adducts are characterized by the interaction between the electron-rich sites of basis and featuring electron holes of acids, and thus, are of considerable interest

for understanding chemical bonding.² This concept is the broadest, and it may be used to classify a large range of events as acid-base reactions. Therefore, discussions of Lewis acidity and basicity appear in almost every textbook of general, organic, and inorganic chemistry.³

Much effort has gone into developing a fundamental measure for estimating Lewis acidity in solids,^{4,5} which has proven to be problematic. The majority of the frequent metric is the strength of basic molecules binding to an acidic site. The most used explanation for this interaction is represented by the electron density in a frontier orbital, resulting from a modest change in the overall number of electrons.⁶

In addition, a number of theoretical efforts have been made to provide qualitative and quantitative insights into these basic notions. From a theoretical standpoint, it has been noted that density functional theory (DFT) offers an effective framework for the creation and investigation of a chemical reactivity theory.⁷ A rising number of gas-phase and theoretical research molecular structures⁸ is not an unchanging aspect of a molecule in this context but rather demonstrates a remarkable phase dependency.⁹

In this study, and following our previous work¹⁰ we will explore in more detail the interactions established between molecules or between molecules and ions. So, in the investigation below, our interest is the Lewis acid-base interactions, which are realized among AlH_3 , and a series of neutral and anionic bases (CO ; H_2O ; NH_3 ; PH_3 ; PCl_3 ; H_2S ; CN^- ; OH^- ; O_2^{2-} ; F^- ; $\text{N}(\text{CH}_3)_3$; N_2 ; N_2H_4 ; N_2H_2 ; $\text{C}_5\text{H}_5\text{N}$; $\text{C}_6\text{H}_5\text{-NH}_2$) stems from the fact that they are quite strong and pseudo-tetrahedral in the coordination chemistry.¹¹ We have examined the nature of the interaction, the bonding strength, and the stability of adducts. Moreover, the concepts of HOMO and LUMO orbitals in describing electron-donor (Lewis-Base) and electron-acceptor (Lewis-Acid) interactions are introduced to estimate and classify the bases according to their nucleophilicity.¹² Thus, the dipolar moment is used as an important property for donor-acceptor adducts as a fundamental measure of charge distribution.

The big request occurs when a Lewis acid-base reaction takes place and leads to the creation of a covalent bond between the acid and the base according to the litera-

¹ Department Matter Sciences, Faculty of Sciences and Technology, University of Abbas Laghrour Khenchela, Algeria

² Laboratory of Materials and Living Chemistry Activity-Reactivity (LCMV-AR); University of Batna1, Algeria

³ Department of Medicine, Faculty of Medicine, University of Batna2, Algeria

✉ hafied_meriem@yahoo.fr

© Aichi M., Hafied M., 2023

ture:¹³ this bond does not necessarily comprise the entire electronic doublet originating from the base, but rather a fraction of it, which may be clarified using various charge transfer methods.¹⁴ The strong interest of our investigation is to provide more information about adduct structures and their charge delocalization. For this purpose, NBO analysis was used to clarify the charge transfer between the donor and the acceptor in Lewis acid-base interaction.

Additionally, the major goal of our current study is to give, by means of computational methods and conceptual DFT, a new view of point to the old definition of Lewis acids or bases as well as the many criteria that influence their interactions. In addition, we have explained the distinction between basicity and nucleophilicity, because in many cases these two concepts are confused by organic chemists.

2. Theory Background

Pearson established the HSAB hypothesis, or acid-base concept, in 1963,¹⁵ and it is commonly used in chemistry to describe compound stability and reaction rate. The concept was introduced in relation to the behavior of Lewis acids (A) and bases (B).



Since the complex molecules or ions, A: B, were considered to be formed from an acceptor electrons A and an electron donor B, since the acid-base complex, A: B, can be an organic molecule, an inorganic molecule, or a complex ion.

The stability of A: B is the result of the acid-base interaction between the two parts. Any insight into the properties of A and B that leads to the formation of a forte binding, would be very helpful. It was well known that there is no one order of acidic force, or of basic strength, which would be vigorous in any case. The “force” here is used in the sense of connection strength formation: that is, a strong acid and a strong base will form the same strong bond.

Based on this classification, Pearson formulated his HSAB principle (hard and soft acids and bases main HSAB) as follows: “Hard acids prefer to react with hard bases and soft acids prefer to react with soft bases”.

2.1. Ionization Potential I

Pearson *et al.* showed that the Mulliken electronegativity (χ) and the hardness (η), analogous to the first- and second-derivatives of energy with respect to a number of electrons, respectively, can be used to measure Lewis acidity with more accuracy. Applying a finite difference approximation for the first derivative and a three-point finite difference approximation for the second derivative

leads to operational definitions in terms of ionization potential (I)¹⁶ and electron affinity (A) as follows:

The ionization potential and electron affinity can be replaced by the HOMO and LUMO energies, respectively, using Koopmans’ theorem within a Hartree-Fock scheme yielding

$$I = -E_{HOMO} \quad (2)$$

$$A = -E_{LUMO} \quad (3)$$

Parr and co-workers¹⁷ interpreted that chemical potential (μ) could be written as the partial derivative of the system’s energy with respect to the number of electrons at a fixed external potential $v(r)$:

$$\chi = -\mu = -\frac{\partial E}{\partial N} = \frac{1}{2} I + A \quad (4)$$

$$\eta = \frac{\partial^2 E}{\partial N^2} = \frac{1}{2} I - A \quad (5)$$

$$\eta = \frac{1}{2} I - A = \frac{1}{2} E_{HOMO} - E_{LUMO} \quad (6)$$

$$\mu = -\frac{1}{2} I + A = -\frac{1}{2} E_{HOMO} + E_{LUMO} \quad (7)$$

$$\chi = \frac{1}{2} I + A = \frac{1}{2} E_{HOMO} + E_{LUMO} \quad (8)$$

Parr *et al.*¹⁷ have introduced the global electrophilicity index (ω) as a measure of energy lowering due to maximal electron flow between a donor and an acceptor in terms of the chemical potential and the hardness as:

$$\omega = \frac{\mu^2}{2\eta} \quad (9)$$

One of the most important global reactivity characteristics is hardness.¹⁸ It is one of the major global reactivity characteristics, with a definition in Eq. (7). I and A are the vertical ionization energy and electron affinity, respectively. Softness (S)¹⁹ is the reciprocal of hardness and is defined as:

$$S = \frac{1}{2\eta} \quad (10)$$

In 2007, Gázquez²⁰ introduced the concepts of the electroaccepting, ω^+ , and electrodonating, ω^- , powers as:

$$\omega^+ = \frac{A^2}{2(I-A)} \quad (11)$$

$$\omega^- = \frac{I^2}{2(1-A)} \quad (12)$$

where ω^+ represents a measure of the propensity of a given system to accept electron density, while ω^- represents the propensity of this system to donate electron density.

In 2008, an empirical (relative) nucleophilicity N index has been proposed for closed-shell organic molecules based on the HOMO energies, E_{HOMO} , obtained within the Kohn-Sham scheme²¹ as an approach to the gas phase, and defined as:

$$N = E_{HOMO} \text{ Nucleophile} - E_{HOMO} \text{ TCE} \quad (13)$$

The nucleophilicity N index is referred to as tetracyanoethylene (TCE), which is the most electrophilic neutral species, the expected least nucleophilic neutral species. This choice allowed the convenient handling of a

nucleophilicity scale of positive values. An analysis of a series of common nucleophilic species participating in polar organic reactions allowed a further classification of organic molecules as strong nucleophiles with $N > 3.0$ eV, moderate nucleophiles with $2.0 \leq N \leq 3.0$ eV, and marginal nucleophiles with $N < 2.0$ eV.¹⁷

In our calculations, we have found the E_{HOMO} (TCE) = -9.121 eV at B3LYP/6-31G(d,p) level.

Moreover, the maximum number of electrons ΔN_{max} that an electrophile can acquire is given by the following expression:¹⁷

$$\Delta N_{max} = -\frac{\mu}{\eta} \quad (14)$$

The maximum charge that each species may accept from the environment which is measured by ΔN_{max} , is almost parallel to the variation in electrophilicity for the whole series of Lewis acid-base adducts. Since the nucleophilicity index obtained as $1/\omega$ was below, we can define the nucleophilicity as $N'' = 1/\omega^-$.

The following methods were adopted for the present study.

$$N' = \frac{1}{\omega} ; \omega = \frac{\mu^2}{2\eta} \quad (15)$$

$$N'' = \frac{1}{\omega^-} ; \omega^- = \frac{I^2}{2(I-A)} \quad (16)$$

2.2. Charge Transfer Analysis (ΔN)

Acids are electron-pair acceptors and bases are electron-pair donors, according to the original Lewis definition 1923.²² The creation of a complex (or adduct, or

coordination compound) A-B reaction (17) is the crucial reaction between a Lewis acid A and a Lewis base B.



Lewis acids and bases are electron-pair acceptors and electron-pair donors, respectively, according to the Lewis theory of acid-base reactions. As a result, a Lewis base can transfer two electrons to a Lewis acid, in general resulting in a product with a coordinated covalent bond. This suggests that Lewis acid-base is a complicated interaction that is influenced by the entire system rather than just the isolated acids and bases.

When two systems, B and A, are combined, electrons move from the lower χ to the higher χ until the chemical potentials are equal. For generalized acid-base reactions, the fractional number of electrons transferred.

$A + :B \rightarrow A:B$, (up to first order) is provided by

$$\Delta N = \frac{(\chi_A - \chi_B)}{2(\eta_A - \eta_B)} \quad (18)$$

The global interactions between AlH₃ and the selected bases of systems have been determined using the parameter ΔN , which represents the fractional number of electrons, transferred from system A to system B. Charge transfer data are presented in Table 1. Generally, electron flows from a less electronegative system to a more electronegative one and this fact along with the definition of ΔN clearly shows that charge transfer values are negative for AlH₃-CO and AlH₃-N₂ showing them as electron donors, and the remains of the adducts ΔN are positive ones, representing them as electron acceptors.

Table 1. Nucleophilicity index N (eV) of chosen bases

Lewis Basis	N (eV)	$\omega = \frac{\mu^2}{2\eta}$ (eV)	$N' = \frac{1}{\omega}$ (eV)	$\omega^- = \frac{I^2}{2(I-A)}$ (eV)	$N'' = \frac{1}{\omega^-}$ (eV)	$\Delta N_{max} = -\frac{\mu}{\eta}$
C=O	0.988	2.987	0.335	5.368	0.186	1.117
CN ⁻	9.625	2.818	0.354	0.014	71.429	-1.111
H ₂ O	1.169	0.977	1.024	3.245	0.308	0.634
H ₂ S	1.995	1.840	0.543	3.601	0.278	1.022
PH ₃	1.634	1.299	0.770	3.345	0.299	0.788
PCl ₃	0.888	4.258	0.235	5.471	0.183	1.659
F	13.691	13.190	0.076	0.328	3.049	-1.287
O ⁻²	26.801	36.634	0.027	6.444	0.155	-2.458
OH	13.484	8.845	0.113	1.372	0.729	-2.257
N ₂	2.510	3.287	0.304	6.064	0.165	1.086
N ₂ H ₄	4.686	0.157	6.369	1.445	0.692	0.303
NH ₃	2.510	0.506	1.976	2.455	0.407	0.476
N(CH ₃) ₃	3.484	0.354	2.825	2.004	0.499	0.423
C ₅ H ₅ N	2.246	2.044	0.489	3.784	0.264	1.202
C ₆ H ₅ -NH ₂	2.575	1.623	0.616	3.263	0.306	0.995
N ₂ H ₂	2.559	0.501	1.996	4.218	0.237	0.500

The maximum charge transfer is estimated in the interaction between AlH_3 and O^{2-} (2.28), between AlH_3 and H_2S with (1.54), and then between AlH_3 and F^- (1.34). The smallest donate charge is between AlH_3 and PCl_3 with (0.00015). Whereas, the energy that follows this charge transfer (Eq. 19) indicates that $\text{AlH}_3\text{-PCl}_3$ is repaired by the great value of energy ($-3.97 \cdot 10^{-8}$).

The reduction in energy caused by this electron transfer from a greater chemical potential (base) to a lower chemical potential (acid)²³ is provided by:

$$\Delta E_{CT} = \frac{(\chi_A - \chi_B)^2}{4(\eta_A + \eta_B)} \quad (19)$$

2.3. Computational Details

Geometry optimizations and frequency calculations of all the molecules and adducts were carried out using density functional theory along with a three-parameter hybrid model (DFT/B3LYP)²⁴ in conjunction with 6-31G(d,p) basis function. All quantum chemical calculations were performed using the Gaussian 09 program.²⁵ All the optimized geometries have no negative vibrational modes showing that all structures are minima on the potential energy surface.

3. Results and Discussion

3.1. Structure of AlH_3 Lewis Acid

AlH_3 or alane is a sterically and electronically unsaturated moiety that reacts readily with a range of Lewis-basis, leading to 1:1 and 1:2 adducts, which are respectively four- or five-coordinate at the Al center.²⁶ The four-coordinate 1:1 adducts of alane ($\text{AlH}_3\text{-B}$) generally adopt a pseudo-tetrahedral configuration at the aluminum center.²⁷

In our results of geometry optimization presented in Fig. 1, the planar geometry of the Lewis acid AlH_3 appears with Al-H = 1.59 Å and the H-Al-H angle is equal to 120°. The map of the electrostatic potential (EP) for the molecular surface of Lewis acid is also illustrated and tends to be between $\pm 7.113 \text{ e}(-2)$. The blue region of EP relates to the positive charge of the aluminum center, nevertheless, the electron-rich sites congregate in the green

hue area of EP and belong to the negative charge of hydrogens. The LUMO orbital is clearly located on the aluminum center that presents the electronic hole. The aim calculated parameters of AlH_3 are presented in Table 2.

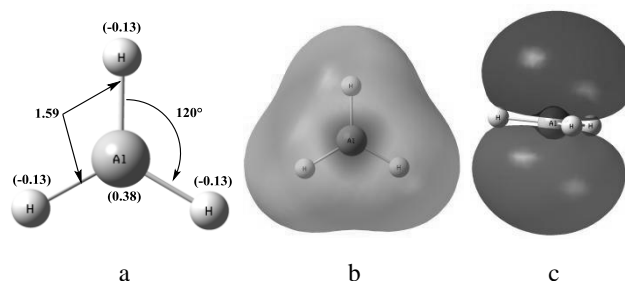


Fig. 1. The planar geometry of AlH_3 (a); the electrostatic potential map for molecular surface (b); the molecular orbital LUMO of AlH_3 (c)

The interactions of AlH_3 with a variety of Lewis-basis suggest that the aluminum center has direct contact with various atoms X of the Lewis-basis (Fig. 2) and that leads to a pseudo-tetrahedral configuration adduct.

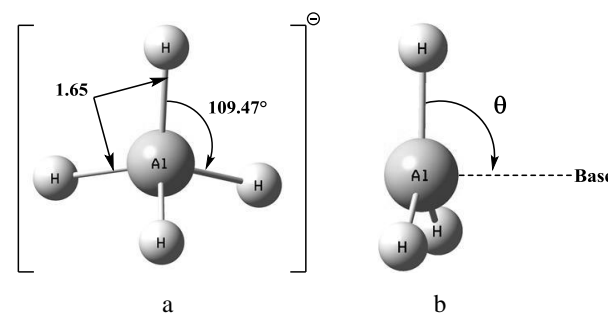


Fig. 2. Tetrahedral (AlH_4^-) (a) and pseudo-tetrahedral $\text{AlH}_3\text{-base}$ geometries (b)

The low ionization energy I shows that the molecule is highly reactive according to Table 3. The increasing order of potential ionization is

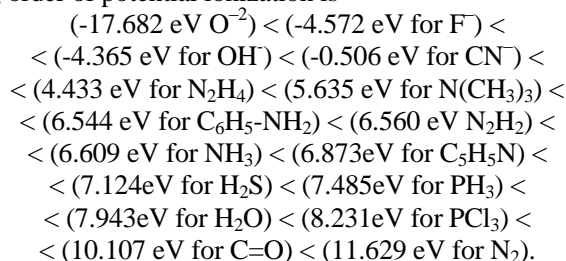
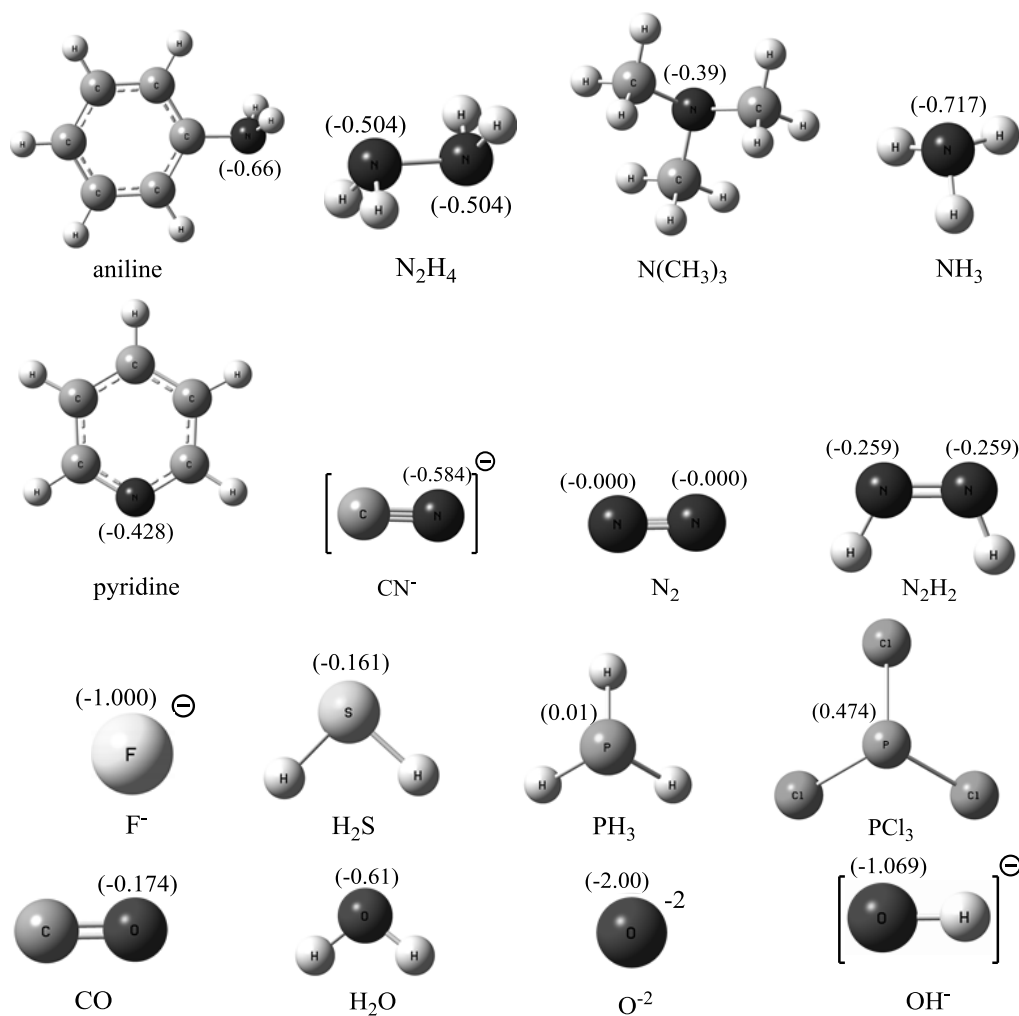


Table 2. Energy and essential parameters of AlH_3 Lewis acid

Et (a.u.)	$I = -E_{HOMO}$ (eV)	$A = -E_{LUMO}$ (eV)	(μ)	χ_A	μ_A	η_A	ω_A	SA
-224.207	8.336	1.936	0.0003	5.136	-5.136	3.2	4.122	0.313

Table 3. The main parameters of chosen Lewis bases

Lewis Basis	Et (a.u.)	$I = -E_{HOMO}$ (eV)	$A = -E_{LUMO}$ (eV)	(μ) (Deby)	$\chi_B = (I+A)/2$	$\mu_B = -\chi$	$\eta_B = (I-A)$	SB=1
C=O	-113.309	10.107	0.592	0.0599	5.349	-5.349	4.789	0.209
CN ⁻	-92.825	-0.506	-9.642	0.5236	-5.074	5.074	4.568	-0.197
H ₂ O	-76.4197	7.943	-1.779	2.0428	3.082	-3.082	4.861	0.206
H ₂ S	-399.392	7.124	0.078	1.3992	3.601	-3.601	3.523	0.284
PH ₃	-343.145	7.485	-0.889	0.9605	3.298	-3.298	4.187	0.239
PCl ₃	-1721.999	8.231	2.039	0.9924	5.135	-5.135	3.096	0.323
F ⁻	-99.754	-4.572	-36.419	0.000	-20.496	20.496	15.924	-15.924
O ²⁻	-74.569	-17.682	-41.943	0.000	-29.813	29.813	12.131	0.082
OH ⁻	-75.726	-4.365	-11.310	1.136	-7.838	7.838	3.473	0.288
N ₂	-109.524	11.629	0.4799	0.000	6.054	-6.054	5.575	0.179
N ₂ H ₄	-111.865	4.433	-2.369	0.0031	1.032	-1.032	3.401	0.294
NH ₃	-56.557	6.609	-2.350	1.8464	2.130	-2.130	4.479	0.223
N(CH ₃) ₃	-174.486	5.635	-2.286	0.5791	1.675	-1.675	3.961	0.252
C ₆ H ₅ N	-248.293	6.873	0.631	2.1848	3.752	-3.752	3.121	0.267
C ₆ H ₅ -NH ₂	-287.607	6.544	-0.0177	1.3150	3.263	-3.263	3.281	0.305
N ₂ H ₂	-110.643	6.560	1.4592	0.000	2.005	-2.005	4.009	0.249


Fig. 3. Structure and Mulliken charge of studied Lewis bases

3.2. Neutral and Anionic-Optimized Lewis Bases

Obtained results show that the more nucleophilic base is O^{-2} (26.801 eV), which is in accordance with the values of the global electrophilicity index ω (36.634) and the electron-donating ω^{-} (6.444). Therefore, the classification of the bases according to their nucleophilicity is: O^{-2} , F^{-} , OH^{-} , CN^{-} , N_2H_4 , $N(CH_3)_3$, $C_6H_5-NH_2$, N_2H_2 , NH_3 , N_2 , C_5H_5N , H_2S , H_2O , PH_3 , CO , PCl_3 . Whereas, their classification according to the electron-donating ω^{-} does not follow the same order: O^{-2} , N_2 , PCl_3 , CO , N_2H_2 , C_5H_5N , H_2S , PH_3 , $C_6H_5-NH_2$, H_2O , NH_3 , $N(CH_3)_3$, N_2H_4 , OH^{-} , F^{-} , CN^{-} .

The nucleophilicity N was estimated theoretically and listed in Table 1 for some anionic and neutral bases (Fig. 3).

The value of ΔN_{max} determines the maximum charge that each basis may accept from the environment. Negative values of ΔN_{max} indicate the maximum charge that the bases can provide.

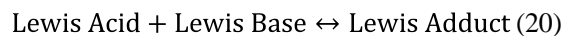
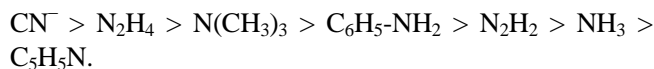
Table 3 shows that the most electronic charge donation is from O^{-2} with ΔN_{max} equal to (-2.458), then OH^{-} can give (-2.257), F^{-} provides (-1.287), and the least contribution is by CN^{-} (-1.111).

3.3. Nucleophilicity Character in Chosen Bases

According to the Lewis definition, Lewis bases have high electron density centers, while Lewis acids have low electron density centers. The electron pair provided by the base is utilized to establish a new sigma bond to the electron-deficient site in the acid. The conversion of the lone pair between the base and the empty orbital of the acid into a covalent bond is known as a Lewis acid-base interaction (Eq. 20).

Nucleophilicity is not a measurement of lone pair reactivity, that is basicity which measures a thermodynamic quality (end-result stability levels of reactants and products), while nucleophilicity measures a kinetic quality (the speed of giving the electron pair). According to this concept, and to clarify the Lewis AlH_3 -base interactions, we have drawn the energy levels of the HOMO orbitals for each interacting base (Fig. 4) that acts as electron pair donors.

O^{-2} presents the highest HOMO energy (17.68 eV) compared to the other bases resulting in the best estimation of nucleophilicity and therefore, we can classify all bases with the order of nucleophilicity: $O^{-2} > F^{-} > OH^{-} >$



$$\Delta G = G_{\text{Adduct}} - G_{\text{Lewis Acid}} - G_{\text{Lewis Base}} \quad (21)$$

$$\Delta H = H_{\text{Adduct}} - H_{\text{Lewis Acid}} - H_{\text{Lewis Base}} \quad (22)$$

3.4. Measurement of Lewis Basicity

The term “basicity” refers to a thermodynamic concept. The location of equilibrium is determined by the respective stabilities of the entities included in the two members of the acid-base Eq. (20) (associated). This may be expressed using the formula $\Delta G = -RT \ln K$, where ΔG is the free standard variation of enthalpy of the reaction.

According to the glossary of terms used in physical organic chemistry published by the International Union of Pure and Applied Chemistry,²⁸ Lewis basicity is defined as follows: the thermodynamic tendency of a substance to act as a Lewis base. Comparative measures of this property are provided by the equilibrium constants for Lewis adduct formation for a series of Lewis bases with a common reference Lewis acid.

A number of researchers²⁸ have proposed measuring Lewis (Brønsted) basicity from the negative enthalpies of the complexation (protonation) reactions (Eq. 20) in order to follow the IUPAC definition of basicity.²⁹ We suggest reserving basicity measurements for Gibbs energies ΔG of adduct formation (protonation) and referring to the relevant enthalpies as “enthalpy of basicity”.

In the Lewis acid-base interaction, Lewis acid steps in through its orbital LUMO to receive the electron doublet. On the other hand, the Lewis base intervenes by orbital HOMO which includes an electronic doublet to give it.

In the Lewis acid-base interaction diagram, the energy gap ΔE_1 between LUMO AlH_3 and HOMO O^{-2} is estimated at 19.618 eV. Depending on the results obtained from the deviations, this value appears to be the highest, which reflects the difficulty of O^{-2} in giving their electronic doublet to the aluminum center. The HOMO of O^{-2} is more energetic than the LUMO of AlH_3 , allowing laborious interaction to place the non-binding doublets of O^{-2} in a lower energy orbital. The energy gap (Fig. 4) indicates that the electron donor power is estimated in the following increasing order: $CN^{-} < N_2H_4 < N(CH_3)_3 < N_2H_2 < C_6H_5-NH_2 < NH_3 < C_5H_5N < H_2S < PH_3 < H_2O < PCl_3 < OH^{-} < F^{-} < CO < N_2 < O^{-2}$.

The above classification makes it possible to give the order of the nucleophilicity of the cited bases, therefore CN^{-} appears as the most nucleophilic while O^{-2} is the least nucleophilic.

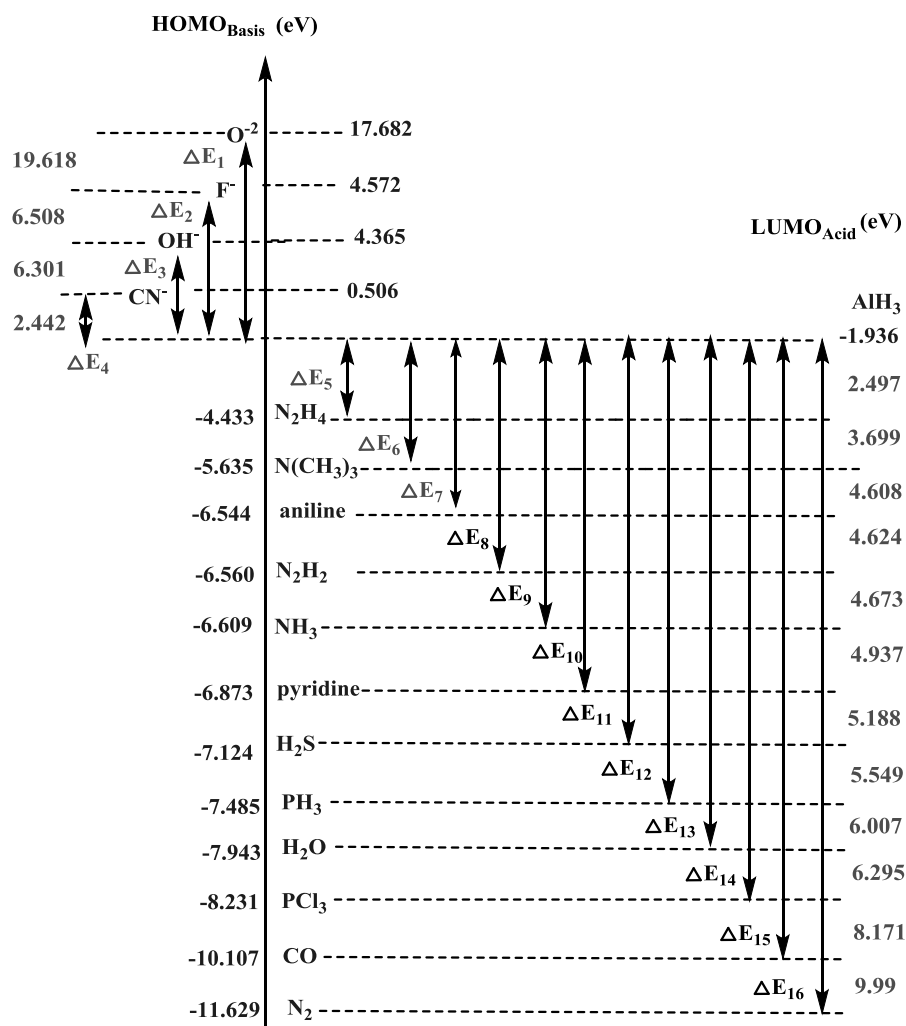


Fig. 4. Estimation of the nucleophilicity *via* the energetic gap ΔE between HOMO-basis and LUMO-AlH₃

3.5. Stability and Charge Transfer of Adducts

3.5.1. Interaction Energy ΔE_{inter}

The system of the two interacting molecules, A and B, is treated as a supermolecule or as a complex and their interaction energy, ΔE , is the energy of the supermolecule or of the complex minus the energies of the isolated molecules.³⁰

$$\Delta E_{inter} = E_{AB} - (E_A + E_B) \quad (23)$$

The lower interaction energy is in accordance with the more stable supermolecule or complex. In our case, the interaction energy for anionic adducts appears as lower one in the case of AlH₃---O₂²⁻ (-20.524 a.u.).

3.5.2. Frontier Molecular Orbitals (FMO)

Molecular orbitals and their properties such as energy are useful for chemists in frontier electron density for

predicting the most reactive systems and also explain several types of reactions in conjugated systems. FMO analysis is widely employed to explain the optical and electronic properties of organic compounds.³¹

The DFT method predicts that the HOMO – LUMO energy gap of obtained adducts, which is very low in the case of AlH₃-N₂H₂ (3.78 eV), leads to lower stability (high chemical reactivity) of the complex and is more polarizable (43.133 a.u.). The large gap is estimated for AlH₃-F⁻ adduct (7.357 eV).

3.5.3. The Angle θ and Al-O Bond

In regular tetrahedral geometry (AlX₄)⁻ the angle θ is estimated at 109.64°. When the base interacts with AlH₃ a pseudo-tetrahedral geometry (AlH₃B) appears and the angle θ value may reflect good parameter stability. On the other hand, the length of Al-O bond is between 1.64 to 1.69 in many compounds with four-coordinate alumi-

num.³² The value that is most similar to regular θ is indicated in $\text{AlH}_3\text{-F}^-$ adduct (109.52°) and the distance Al-F^- is equal to 1.14\AA .

Whereas, in $\text{AlH}_3\text{-O}^{2-}$ adduct the bond length between Al and O^{2-} is 1.69\AA and θ is equal to 118.62° . In

addition, the values of θ in $\text{AlH}_3\text{-CN}^-$ and $\text{AlH}_3\text{-OH}^-$ are 106.98° and 111.47° , respectively. The lengths of the Al-CN^- (1.94\AA) and Al-OH^- (1.80\AA) bonds are optimal (Table 4). Except for $\text{AlH}_3\text{-pyridine}$ and $\text{AlH}_3\text{-aniline}$, the rest of the structures have an angle θ less than 100° .

Table 4. Energetic parameters of AlH_3 -base adducts

Adducts	$\theta(^\circ)$	E_t (a.u.)	E_{HOMO} (eV)	E_{LUMO} (eV)	$\Delta E_{HOMO-LUMO}$ (eV)	ν (cm^{-1}) stretching	$\text{AlH}_3\text{-Base}$ (\AA)	ΔE_{inter} (a.u.)
$\text{AlH}_3\text{-CO}$	93.14	-357.523	-8.005	-1.807	6.198	121.58	2.38	-20.007
$\text{AlH}_3\text{-CN}^-$	106.98	-337.144	-2.154	3.423	5.568	491.19	1.94	-20.112
$\text{AlH}_3\text{-H}_2\text{O}$	97.67	-320.664	-7.287	-0.694	6.593	368.08	2.05	-20.038
$\text{AlH}_3\text{-OH}^-$	111.47	-320.129	-1.221	5.416	6.637	679.88	1.80	-20.196
$\text{AlH}_3\text{-H}_2\text{S}$	97.99	-643.617	-7.575	-0.604	6.971	203.17	2.61	-20.020
$\text{AlH}_3\text{-NH}_3$	99.27	-300.815	-7.108	-0.190	6.918	406.18	2.09	-20.051
$\text{AlH}_3\text{-PH}_3$	96.82	-587.374	-7.526	-0.122	7.404	229.14	2.58	-20.022
$\text{AlH}_3\text{-PCl}_3$	93.43	-1966.215	-8.158	-2.694	5.464	138.89	2.63	-20.009
$\text{AlH}_3\text{-N}(\text{CH}_3)_3$	99.93	-418.742	-7.028	0.623	7.66	279.44	2.09	-20.049
$\text{AlH}_3\text{-F}^-$	109.52	-344.177	-1.658	5.699	7.357	722.51	1.14	-20.216
$(\text{AlH}_3)_2\text{N}_2\text{H}_4$	98.12	-356.125	-7.213	0.0005	7.214	390.00	2.09	-20.053
$\text{AlH}_3\text{-O}^{2-}$	118.62	-319.300	6.067	10.968	4.901	930.51	1.69	-20.524
$\text{AlH}_3\text{-N}_2$	93.78	-353.471	-8.027	-2.174	5.853	172.30	2.27	-19.74
$\text{AlH}_3\text{-C}_5\text{H}_5\text{N}$	100.73	-492.547	-6.781	-2.033	4.748	276.83	2.70	-20.047
$\text{AlH}_3\text{-C}_6\text{H}_5\text{NH}_2$	100.40	-531.863	-6.909	-0.626	6.283	368.39	2.11	-20.049
$\text{AlH}_3\text{-N}_2\text{H}_2$	94.25	-354.877	-7.302	-3.516	3.786	358.12	2.10	-20.027

Optimized structures of all adducts with Mullikan atomic charge and the main bond lengths are shown in Fig. 5. AlH_3 -base bond length (\AA) and the corresponding IR stretching frequency (cm^{-1}), dipolar moment and induced dipolar moment (Deby), the fractional charge transfer (ΔN), the interaction energy E_{inter} , the polarizability α , the enthalpy ΔH adduct (kJ/mol),

and the free Gibbs energies ΔG_{adduct} (kJ/mol) calculated at the same level at $T = 298.15\text{ K}$ are listed in Table 5. The order of stability in the considered adducts is:

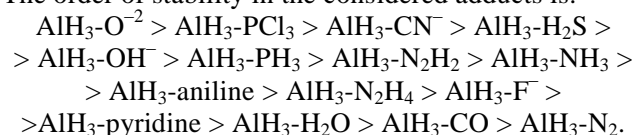


Table 5. Dipolar Moment (μ), Polarizability (α), ΔG_{Adduct} , ΔH_{Adduct} , $\Delta\mu_{ind}$, ΔN , and ΔE_{CT}

Adduct	(μ) (Deby)	(α) (a.u.)	ΔG_{Adduct} (KJ/mol)	ΔH (kJ/mol)	$\Delta\mu_{ind}$ (Deby)	ΔN	ΔE_{CT} (e.V)
$\text{AlH}_3\text{-CO}$	1.610	35.23	70.947	7.285	1.551	-0.061	-0.028
$\text{AlH}_3\text{-CN}^-$	0.334	41.313	46.615	7.758	-0.189	0.657	-3.355
$\text{AlH}_3\text{-H}_2\text{O}$	4.862	29.989	64.752	9.150	2.783	0.127	-0.131
$\text{AlH}_3\text{-OH}^-$	2.903	32.201	47.430	11.073	1.767	0.972	-0.599
$\text{AlH}_3\text{-H}_2\text{S}$	3.750	43.595	47.150	10.722	2.351	1.535	-0.088
$\text{AlH}_3\text{-NH}_3$	5.689	33.578	52.125	13.426	3.842	0.196	-0.294
$\text{AlH}_3\text{-PH}_3$	4.284	51.018	47.777	10.391	3.323	0.146	-0.114
$\text{AlH}_3\text{-PCl}_3$	1.458	84.849	45.607	8.347	0.465	0.15×10^{-3}	-3.97×10^{-8}
$\text{AlH}_3\text{-N}(\text{CH}_3)_3$	5.403	64.998	61.291	13.827	4.824	0.569	-0.569
$\text{AlH}_3\text{-F}^-$	1.861	27.918	57.738	4.807	1.861	1.340	-8.589
$(\text{AlH}_3)_2\text{N}_2\text{H}_4$	5.375	41.266	56.551	12.305	5.372	0.622	-0.638
$\text{AlH}_3\text{-O}^{2-}$	1.877	39.537	30.209	-2.153	1.877	2.279	-19.92
$\text{AlH}_3\text{-N}_2$	1.834	36.479	89.386	7.937	1.834	-0.105	-0.024
$\text{AlH}_3\text{-C}_5\text{H}_5\text{N}$	7.384	79.109	57.771	8.610	5.199	0.199	-0.071
$\text{AlH}_3\text{-C}_6\text{H}_5\text{NH}_2$	5.530	89.628	53.391	15.015	4.215	0.289	-0.169
$\text{AlH}_3\text{-N}_2\text{H}_2$	5.919	43.133	52.008	7.432	5.919	0.434	-0.339

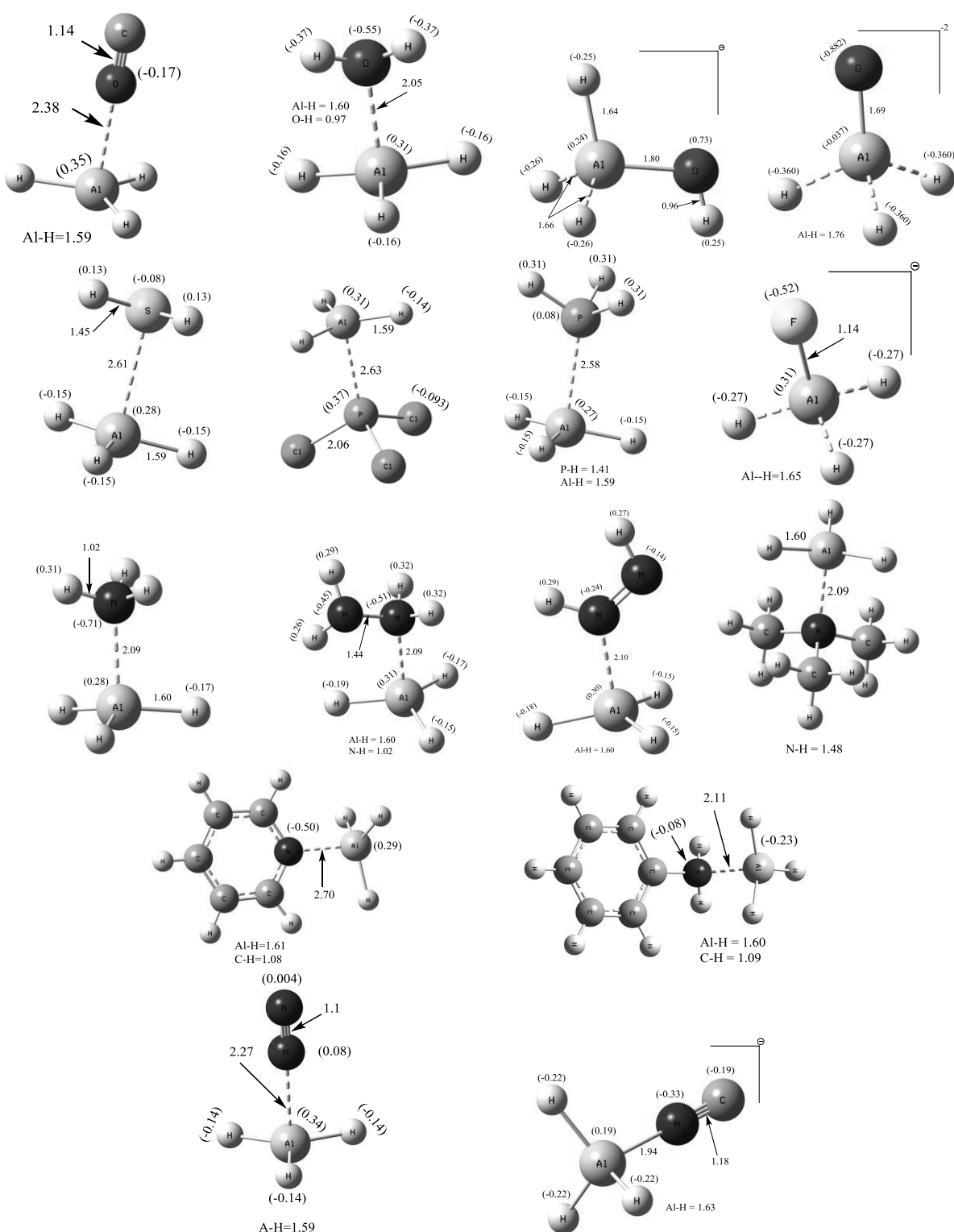
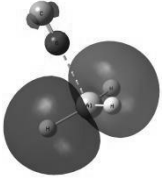
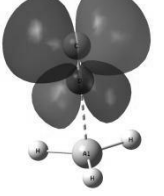
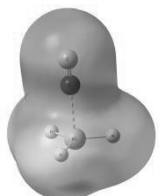
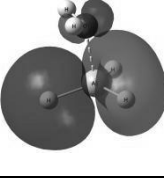
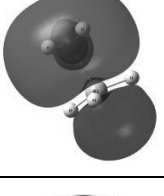
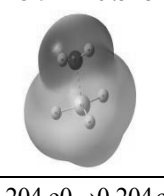
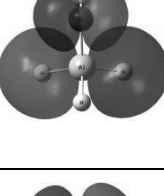
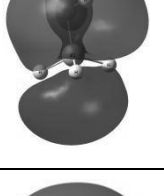
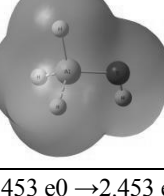
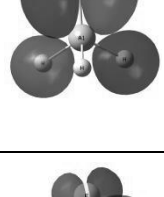
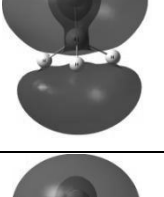
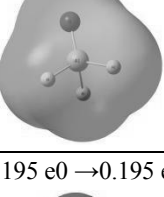
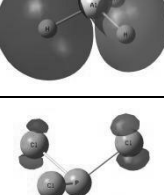
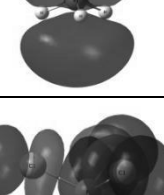
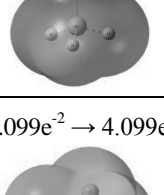
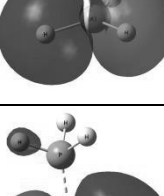
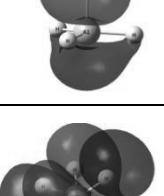
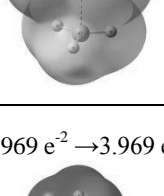
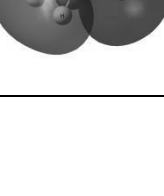
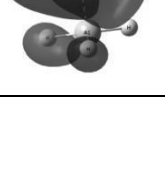
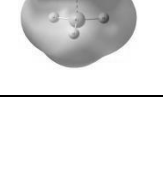


Fig. 5. Optimized adducts at B3LYP/6-31G(d,p) level

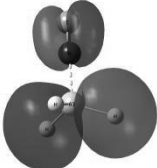
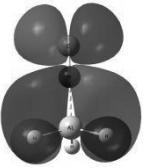

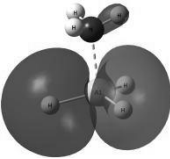
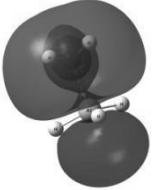
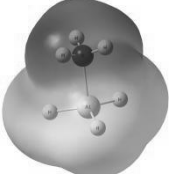
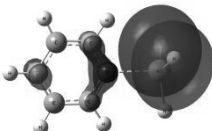
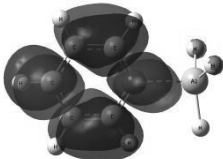
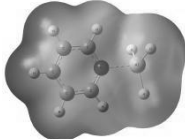
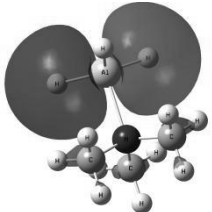
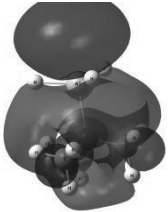
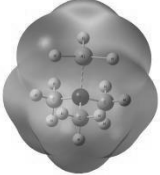
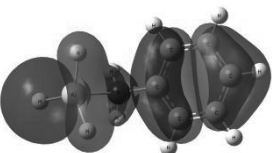
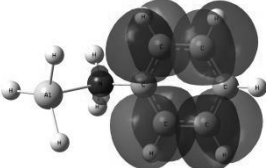

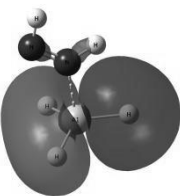
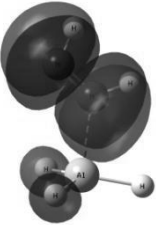
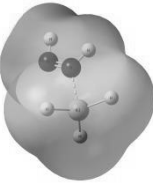
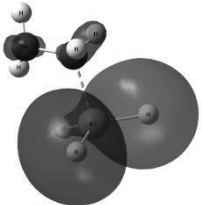
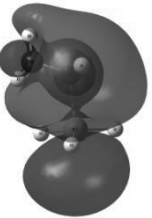
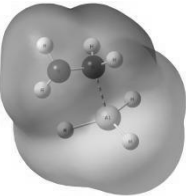
Table 6 shows the frontier orbitals (HOMO and LUMO plots) and the estimation of the energetic gap

$\Delta E_{HOMO-LUMO}$. Besides, the electrostatic surface potential map is also displayed for all adducts.

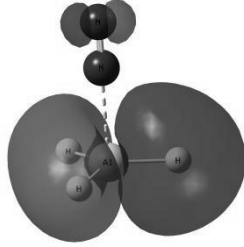
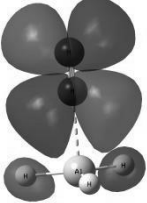
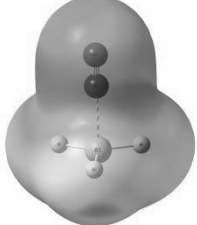
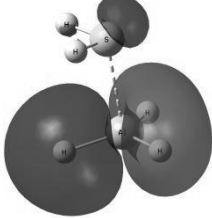
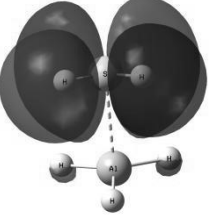
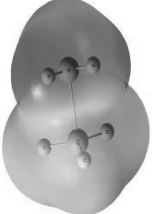
Table 6. The HOMO and LUMO plots, $\Delta E_{HOMO-LUMO}$ (eV) and the electrostatic potential surface map (EPS)

Adducts	HOMO (eV)	LUMO	$\Delta E_{HOMO-LUMO}$ (eV)	EPS
1	2	3	4	5
AlH_3-CO			6.198	-4.612e-2 \rightarrow 4.612 e-2 
AlH_3-H_2O			6.592	-9.548 e-2 \rightarrow 9.548 e-2 
AlH_3-OH			6.637	-0.204 e0 \rightarrow 0.204 e0 
AlH_3-O^{2-}			4.901	-2.453 e0 \rightarrow 2.453 e0 
AlH_3-F^-			7.356	-0.195 e0 \rightarrow 0.195 e0 
AlH_3-PCl_3			5.463	-4.099e-2 \rightarrow 4.099e-2 
AlH_3-PH_3			7.403	-3.969 e-2 \rightarrow 3.969 e-2 

Continuation of Table 6

1	2	3	4	5
$\text{AlH}_3\text{-CN}^-$			5.577	-0.174 e ⁰ → 0.174 e ⁰ 
$\text{AlH}_3\text{-NH}_3$			6.918	-7.022 e ⁻² → 7.022 e ⁻² 
$\text{AlH}_3\text{-C}_5\text{H}_5\text{N}$			4.748	-4.353 e ⁻² → 4.353 e ⁻² 
$\text{AlH}_3\text{-N(CH}_3)_3$			7.651	-3.706 e ⁻² → 3.706 e ⁻² 
$\text{AlH}_3\text{-C}_6\text{H}_5\text{-NH}_2$			6.282	-6.401 e ⁻² → 6.401 e ⁻² 
$\text{AlH}_3\text{-N}_2\text{H}_2$			3.787	-0.101 e ⁰ → 0.101 e ⁰ 
$\text{AlH}_3\text{-N}_2\text{H}_4$			7.214	-7.486 e ⁻² → 7.486 e ⁻² 

Continuation of Table 6

1	2	3	4	5
$\text{AlH}_3\text{-N}_2$			5.852	$-4.003e^{-2} \rightarrow 4.003e^{-2}$ 
$\text{AlH}_3\text{-H}_2\text{S}$			6.971	$-5.274e^{-2} \rightarrow 5.274e^{-2}$ 

By comparing the $\Delta E_{HOMO-LUMO}$ values of different adducts, we may categorize the structures as follows: $\text{AlH}_3\text{-N}(\text{CH}_3)_3 > \text{AlH}_3\text{-PH}_3 > \text{AlH}_3\text{-F}^- > \text{AlH}_3\text{-N}_2\text{H}_4 > \text{AlH}_3\text{-H}_2\text{S} > \text{AlH}_3\text{-NH}_3 > \text{AlH}_3\text{-OH}^- > \text{AlH}_3\text{-H}_2\text{O} > \text{AlH}_3\text{-C}_6\text{H}_5\text{-NH}_2 > \text{AlH}_3\text{-CO} > \text{AlH}_3\text{-N}_2 > \text{AlH}_3\text{-CN}^- > \text{AlH}_3\text{-PCl}_3 > \text{AlH}_3\text{-O}^{-2} > \text{AlH}_3\text{-C}_5\text{H}_5\text{N} > \text{AlH}_3\text{-N}_2\text{H}_2$. The highest value is associated with $\text{AlH}_3\text{-N}(\text{CH}_3)_3$ (7.65 eV) and helps to understand the difficulty of charge transfer.

The electrostatic potential of the molecule (MEP) is still a helpful guide in determining a molecule's reactivity toward positively or negatively charged structures. MEP is usually displayed by projecting its values onto a surface that reflects the boundaries of the molecules.

In the electrostatic potential map (Table 6) the total density depicts the localization of charges surrounding the atoms; it should be noticed that the richness of electrons is concentrated in the red and yellow color regions, and the blue region of EPS relates to the positive charge.

EPS can be used to distinguish the electron-rich (which undergoes electrophilic attack) and electron-poor (which undergoes nucleophilic attack) regions on the surface, making it a useful tool in exploiting the correlation between molecular structure and the relationship of physicochemical properties of molecules.

The largest interval of electron density has been found for $\text{AlH}_3\text{-H}_2\text{O}$ structure, and it tends to be between $\pm 9.548 e^{-2}$. While the restraint interval of electron density characterizes $\text{AlH}_3\text{-N}_2\text{H}_2$ adduct and it tends toward $\pm 0.101 e0$.

3.6. Charge Transfer in Lewis Acid-Base Adducts

3.6.1. Induced Dipolar Moment

Dipolar moment is an important property for donor-acceptor complexes as a fundamental measure of charge distribution in the gas phase or in solution.³³

In this work, we present the calculated values of the dipolar moment, at B3LYP/6-31G(d,p) level of the theory, for sixteen bases and Lewis acid-base adducts. The obtained results are used to examine the relationship between the dipolar moment induced by complexation and the bond length of the donor-acceptor system. The quantity of charge transfer can be used to understand the Lewis acid-base adducts bond.

Generally, the induced dipolar moment of an adduct AB (μ_{AB}) obtained from the dipolar moment of Lewis acid A (μ_A) and Lewis base B (μ_B) can be given by the variation:³³

$$\Delta\mu_{ind} = \mu_{AB} - \mu_A - \mu_B \quad (24)$$

The Mulliken charge analysis and the natural bond orbital (NBO) are important tools for studying intermolecular and intramolecular interactions, as well as a good starting point for investigating net charge transfer in molecular systems.

3.6.2. The NBO Theory

NBO analysis has already proved to be an effective tool for the chemical interpretation of hyperconjugative interactions and electron density transfer from the filled lone-pair electron. The orbital natural binding (NBO) method of Weinhold *et al.*³³ provides a suitable scheme for the analysis of Lewis acid-base interactions because it

emphasizes the computation of electron density delocalization in vacant orbitals.

An interesting example is provided by the NBO analysis of the water dimer $\text{H}_2\text{O}\dots\text{H-O-H}$, where the left and right molecules act like the Lewis base and Lewis acid, respectively. The interaction energy is broken down into charge transfer (CT) and no charge transfer (NCT) as follows:

$$\Delta E = \Delta E_{NCT} + \Delta E_{CT} \quad (25)$$

For each donor NBO (i) and acceptor NBO (j), the stabilization energy (E_2) associated with the delocalization $i \rightarrow j$ is given by:

$$E_2 = \Delta E_{ij} = q_i \frac{F_{ij}^2}{\varepsilon_i - \varepsilon_j} \quad (26)$$

In our case, the significant interactions in the calculated adduct structures are listed in Table 7.

Table 7. Principal charge delocalization of dominant interaction donor–acceptor of AlH_3 —Bases adducts

Adducts	Donor (i)	Occupancy	Acceptor (j)	Occupancy	Interaction type	$E^{(2)}$ (kJ/mol)
1	2	3	4	5	6	7
$\text{AlH}_3\text{-CO}$	LP(O)	1.9363	LP*(Al)	0.0584	LP(O) \rightarrow LP*(Al)	102.20
	$\sigma_{\text{O,C}}$	1.9992	LP*(Al)	0.0584	$\sigma_{\text{O,C}}$ \rightarrow LP*(Al)	11.29
$\text{AlH}_3\text{-CN}^-$	LP(C1)	1.9655	$\sigma_{\text{N2-Al3}}^*$	0.0454	LP(C1) \rightarrow $\sigma_{\text{N2-Al3}}^*$	8.32
	$\sigma_{\text{N2-Al}}$	1.9863	$\sigma_{\text{C1-N2}}^*$	0.0065	$\sigma_{\text{N2-Al}}$ \rightarrow $\sigma_{\text{C1-N2}}^*$	5.01
			$\sigma_{\text{Al-H4}}^*$	0.0188	$\sigma_{\text{N2-Al}}$ \rightarrow $\sigma_{\text{Al-H4}}^*$	5.01
			$\sigma_{\text{Al-H5}}^*$	0.0187	$\sigma_{\text{N2-Al}}$ \rightarrow $\sigma_{\text{Al-H5}}^*$	5.01
			$\sigma_{\text{Al-H6}}^*$	0.0187	$\sigma_{\text{N2-Al}}$ \rightarrow $\sigma_{\text{Al-H6}}^*$	50.91
$\text{AlH}_3\text{-O}^{2-}$	$\sigma_{\text{Al-O5}}$	1.9343	$\sigma_{\text{Al-H4}}^*$	0.0828	$\sigma_{\text{Al-O5}}$ \rightarrow $\sigma_{\text{Al-H4}}^*$	87.86
			$\sigma_{\text{Al-H2}}^*$	0.0828	$\sigma_{\text{Al-O5}}$ \rightarrow $\sigma_{\text{Al-H2}}^*$	65.79
			$\sigma_{\text{Al-H3}}^*$	0.0828	$\sigma_{\text{Al-O5}}$ \rightarrow $\sigma_{\text{Al-H3}}^*$	66.04
$\text{AlH}_3\text{-OH}$	$\sigma_{\text{Al-O5}}$	1.9888	$\sigma_{\text{Al-H2}}^*$	0.0260	$\sigma_{\text{Al-O5}}$ \rightarrow $\sigma_{\text{Al-H2}}^*$	7.35
			$\sigma_{\text{Al-H3}}^*$	0.0459	$\sigma_{\text{Al-O5}}$ \rightarrow $\sigma_{\text{Al-H3}}^*$	5.14
			$\sigma_{\text{Al-H4}}^*$	0.0459	$\sigma_{\text{Al-O5}}$ \rightarrow $\sigma_{\text{Al-H4}}^*$	5.14
			$\sigma_{\text{O5-H6}}^*$	0.0035	$\sigma_{\text{Al-O5}}$ \rightarrow $\sigma_{\text{O5-H6}}^*$	10.45
$\text{AlH}_3\text{-F}^-$	$\sigma_{\text{Al-F5}}$	1.9923	$\sigma_{\text{Al-H2}}^*$	0.0443	$\sigma_{\text{Al-F5}}$ \rightarrow $\sigma_{\text{Al-H2}}^*$	6.48
			$\sigma_{\text{Al-H3}}^*$	0.0443	$\sigma_{\text{Al-F5}}$ \rightarrow $\sigma_{\text{Al-H3}}^*$	6.48
			$\sigma_{\text{Al-H4}}^*$	0.0443	$\sigma_{\text{Al-F5}}$ \rightarrow $\sigma_{\text{Al-H4}}^*$	6.48
			$\sigma_{\text{Al-H4}}^*$	0.0443	LP3(F5) \rightarrow $\sigma_{\text{Al-H4}}^*$	32.98
$\text{AlH}_3\text{-H}_2\text{O}$	$\sigma_{\text{Al-O5}}$	1.9910	$\sigma_{\text{Al-H2}}^*$	0.0158	$\sigma_{\text{Al-O5}}$ \rightarrow $\sigma_{\text{Al-H2}}^*$	6.10
			$\sigma_{\text{Al-H3}}^*$	0.0158	$\sigma_{\text{Al-O5}}$ \rightarrow $\sigma_{\text{Al-H3}}^*$	6.10
			$\sigma_{\text{Al-H4}}^*$	0.0206	$\sigma_{\text{Al-O5}}$ \rightarrow $\sigma_{\text{Al-H4}}^*$	5.48
$\text{AlH}_3\text{-H}_2\text{S}$	$\sigma_{\text{Al1-S5}}$	1.9904	$\sigma_{\text{Al-H2}}^*$	0.0165	$\sigma_{\text{Al1-S5}}$ \rightarrow $\sigma_{\text{Al1-H2}}^*$	6.02
			$\sigma_{\text{Al-H3}}^*$	0.0165	$\sigma_{\text{Al1-S5}}$ \rightarrow $\sigma_{\text{Al1-H3}}^*$	6.02
			$\sigma_{\text{Al-H4}}^*$	0.0185	$\sigma_{\text{Al1-S5}}$ \rightarrow $\sigma_{\text{Al1-H4}}^*$	5.14
$\text{AlH}_3\text{-PH}_3$	$\sigma_{\text{Al-P5}}$	1.9838	$\sigma_{\text{Al-H2}}^*$	0.0142	$\sigma_{\text{Al-P5}}$ \rightarrow $\sigma_{\text{Al1-H2}}^*$	6.23
			$\sigma_{\text{Al-H3}}^*$	0.0142	$\sigma_{\text{Al-P5}}$ \rightarrow $\sigma_{\text{Al1-H3}}^*$	6.23
			$\sigma_{\text{Al-H4}}^*$	0.0142	$\sigma_{\text{Al-P5}}$ \rightarrow $\sigma_{\text{Al1-H4}}^*$	6.23
$\text{AlH}_3\text{-PCl}_3$	$\sigma_{\text{Al-P5}}$	1.9332	$\sigma_{\text{Al-H2}}^*$	0.0176	$\sigma_{\text{Al-P5}}$ \rightarrow $\sigma_{\text{Al1-H2}}^*$	5.39
			$\sigma_{\text{Al-H3}}^*$	0.0176	$\sigma_{\text{Al-P5}}$ \rightarrow $\sigma_{\text{Al1-H3}}^*$	5.39
			$\sigma_{\text{Al-H4}}^*$	0.0176	$\sigma_{\text{Al-P5}}$ \rightarrow $\sigma_{\text{Al1-H4}}^*$	5.39
			$\sigma_{\text{P5-Cl6}}^*$	0.1568	$\sigma_{\text{Al-P5}}$ \rightarrow $\sigma_{\text{P5-Cl6}}^*$	23.07
			$\sigma_{\text{P5-Cl7}}^*$	0.1569	$\sigma_{\text{Al-P5}}$ \rightarrow $\sigma_{\text{P5-Cl7}}^*$	23.07
			$\sigma_{\text{P5-Cl8}}^*$	0.1569	$\sigma_{\text{Al-P5}}$ \rightarrow $\sigma_{\text{P5-Cl8}}^*$	23.07
$\text{AlH}_3\text{-NH}_3$	$\sigma_{\text{Al-N5}}$	1.9864	$\sigma_{\text{Al-H2}}^*$	0.0134	$\sigma_{\text{Al-N5}}$ \rightarrow $\sigma_{\text{Al-H2}}^*$	5.31
			$\sigma_{\text{Al-H3}}^*$	0.0134	$\sigma_{\text{Al-N5}}$ \rightarrow $\sigma_{\text{Al-H3}}^*$	5.31
			$\sigma_{\text{Al-H4}}^*$	0.0134	$\sigma_{\text{Al-N5}}$ \rightarrow $\sigma_{\text{Al-H4}}^*$	5.31
$\text{AlH}_3\text{-N}_2$	$\sigma_{\text{Al-N5}}$	1.9900	$\sigma_{\text{Al-H2}}^*$	0.0163	$\sigma_{\text{Al-N5}}$ \rightarrow $\sigma_{\text{Al-H2}}^*$	4.81
			$\sigma_{\text{Al-H3}}^*$	0.0163	$\sigma_{\text{Al-N5}}$ \rightarrow $\sigma_{\text{Al-H3}}^*$	4.81
			$\sigma_{\text{Al-H4}}^*$	0.0163	$\sigma_{\text{Al-N5}}$ \rightarrow $\sigma_{\text{Al-H4}}^*$	4.81
			$\text{RY}^*_{(\text{N5})}$	0.0014	LP(N6) \rightarrow $\text{RY}^*_{(\text{N5})}$	43.64
			$\sigma_{\text{Al-N5}}^*$	0.0450	LP(N6) \rightarrow $\sigma_{\text{Al-N5}}^*$	17.77
$\text{AlH}_3\text{-N}_2\text{H}_4$	$\sigma_{\text{Al-N5}}$	1.9767	$\sigma_{\text{Al-H2}}^*$	0.0134	$\sigma_{\text{Al-N5}}$ \rightarrow $\sigma_{\text{Al-H2}}^*$	5.31
			$\sigma_{\text{Al-H3}}^*$	0.0139	$\sigma_{\text{Al-N5}}$ \rightarrow $\sigma_{\text{Al-H3}}^*$	5.56
			$\sigma_{\text{Al-H4}}^*$	0.0132	$\sigma_{\text{Al-N5}}$ \rightarrow $\sigma_{\text{Al-H4}}^*$	4.31

Continuation of Table 7

1	2	3	4	5	6	7
AlH ₃ -N ₂ H ₂	$\sigma_{\text{Al-N5}}$	1.9697	$\sigma_{\text{Al-H2}}^*$ $\sigma_{\text{Al-H3}}^*$ $\sigma_{\text{Al-H4}}^*$	0.0143 0.0133 0.0133	$\sigma_{\text{Al-N5}} \rightarrow \sigma_{\text{Al-H2}}^*$ $\sigma_{\text{Al-N5}} \rightarrow \sigma_{\text{Al-H3}}^*$ $\sigma_{\text{Al-N5}} \rightarrow \sigma_{\text{Al-H4}}^*$	6.35 4.81 4.81
AlH ₃ -N(CH ₃) ₃	$\sigma_{\text{Al-N5}}$	1.9367	$\sigma_{\text{Al-H2}}^*$ $\sigma_{\text{Al-H3}}^*$ $\sigma_{\text{Al-H4}}^*$ $\sigma_{\text{C6-H9}}^*$ $\sigma_{\text{C7-H12}}^*$ $\sigma_{\text{C8-H15}}^*$	0.0137 0.0137 0.0137 0.0160 0.0160 0.0160	$\sigma_{\text{Al-N5}} \rightarrow \sigma_{\text{Al-H2}}^*$ $\sigma_{\text{Al-N5}} \rightarrow \sigma_{\text{Al-H3}}^*$ $\sigma_{\text{Al-N5}} \rightarrow \sigma_{\text{Al-H4}}^*$ $\sigma_{\text{Al-N5}} \rightarrow \sigma_{\text{C6-H9}}^*$ $\sigma_{\text{Al-N5}} \rightarrow \sigma_{\text{C7-H12}}^*$ $\sigma_{\text{Al-N5}} \rightarrow \sigma_{\text{C8-H15}}^*$	4.14 4.14 4.14 18.43 18.43 18.43
AlH ₃ -C ₅ H ₅ N	LP(N5) $\sigma_{\text{N5-C6}}$ $\pi_{\text{N5-C10}}$	1.8054 1.9857 1.7582	LP [*] (Al1) LP [*] (Al1) $\pi_{\text{C6-C7}}^*$ $\pi_{\text{C8-C9}}^*$	0.1447 0.1447 0.0196 0.2927	LP(N5) \rightarrow LP [*] (Al) $\sigma_{\text{N5-C6}} \rightarrow \text{LP}^*(\text{Al})$ $\pi_{\text{N5-C10}} \rightarrow \pi_{\text{C6-C7}}^*$ $\pi_{\text{N5-C10}} \rightarrow \pi_{\text{C8-C9}}^*$	290.80 29.34 260.33 380.76
AlH ₃ -C ₆ H ₅ -NH ₂	LP(N5) $\sigma_{\text{N-H13}}$ $\pi_{\text{C2-C3}}$	1.8096 1.9864 1.6722	LP [*] (Al) LP [*] (Al) $\pi_{\text{C1-C6}}^*$	0.1302 0.1302 0.3280	LP(N) \rightarrow LP [*] (Al) $\sigma_{\text{N-H13}} \rightarrow \text{LP}^*(\text{Al})$ $\pi_{\text{C2-C3}} \rightarrow \pi_{\text{C1-C6}}^*$	244.03 25.49 1 021.55

E⁽²⁾ refers energy of interaction

In AlH₃-CN⁻, the occupancy of Al-N bond is 1.986, which is mainly obtained from the lone pair of the N atom. The intramolecular interaction of LP(C1) \rightarrow $\sigma_{\text{N2-Al}}$ and $\sigma_{\text{N2-Al}} \rightarrow \sigma_{\text{Al-H6}}^*$ with stabilization energies of 8.31 kJ/mol and (50.91 kJ/mol), respectively. Similarly, intramolecular interaction from $\sigma_{\text{N2-Al}}$ to $\sigma_{\text{Al-H6}}^*$ leading to the stabilization energy of (66.04 kJ/mol).

The strong intramolecular interactions appear in AlH₃-O²⁻ where the occupancy of Al-O is 1.934. $\sigma_{\text{Al-O5}} \rightarrow \sigma_{\text{Al-H4}}^*$; $\sigma_{\text{Al-O5}} \rightarrow \sigma_{\text{Al-H2}}^*$ and $\sigma_{\text{Al-O5}} \rightarrow \sigma_{\text{Al-H3}}^*$ going to lead stabilization energies 87.86; 65.79; 66.04 kJ/mol) separately.

In the major cases, the partial charge transfer from the formed Al-base goes to the non-bonding $\sigma_{\text{Al-H}}$ orbital, while in AlH₃-N₂ the lone pair nitrogen atom LP(N₆) with a high occupation number of 1.9837 and p-character (~67%), donates an electron to the antibonding $\sigma_{\text{Al-N5}}^*$ with 17.76 kJ/mol energy of interaction.

It is noted that in AlH₃-pyridine and AlH₃-aniline, the lone pair Lp(N5) of nitrogen atom with p-character (74.95%) has an occupied number of 1.8054 and 1.8096, respectively. The interactions LP(N5) \rightarrow LP^{*}(Al) are with considerably high stabilization energies (290.84 and 244.03 kJ/mol, respectively). The adduct systems are stabilized as a result of the intramolecular charge transfer. The $\pi \rightarrow \pi^*$ interactions occur between the bonding $\pi_{\text{N5-C10}}$ and antibonding orbitals $\pi_{\text{C6-C7}}^*$ as well as the bonding $\pi_{\text{C2-C3}}$ and antibonding orbitals $\pi_{\text{C1-C6}}^*$, with a strong stabilization energy of 380.76 and 1021.55 kJ/mol, respectively.

In comparison, $\sigma \rightarrow \sigma^*$ interactions have the lowest delocalization energy compared with $\pi \rightarrow \pi^*$ interactions. As a result, the σ bonds have higher electron density occupancy than the π bonds.

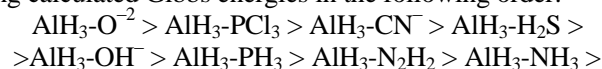
4. Conclusions

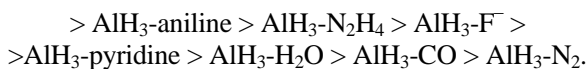
In this investigation, using at DFT/B3LYP/6-31G(d,p) level of theory, we have described the concept of the partial dative bond which can be established in the Lewis acid-base interaction. Besides, this work provides detailed insights into the electronic structure properties using conceptual DFT to establish the primary parameters affecting the formation of this bond and the stability of the resulting adducts.

The charge transfer plays a crucial role in describing dative bond formation. The values of ΔN , ΔN_{max} , the energy following the charge transfer ΔE , the electrodonating ω^- , and the potential ionization permit quantifying and classifying O²⁻ as the most nucleophilic compared to the other studied systems.

The interactions that occur are able to explain the reactivity of the lone pairs and their participation in the formation of a new bonding that appears in the Lewis acid-base interaction. Calculating of the energetic gap between HOMO of the bases and the LUMO of AlH₃ indicate that CN⁻ has the power lone pair donation by the lowest gap ($\Delta E = 2.442$ eV).

We were able to describe the produced adducts using calculated Gibbs energies in the following order:





Acknowledgments

Calculations were realized in the laboratory of materials and living chemistry activity-reactivity (LCMV-AR); Department of Chemistry, Faculty of Matter Sciences, Batna1 University, Algeria. The authors are grateful to Prof. Messaoudi Abdelatif, the head of research, for his useful comments.

References

- [1] Hankinson, D.J.; Almlöf, J.; Leopold, K.R. A Direct Comparison between Structure Correlations and Reaction Paths. *J. Phys. Chem.* **1996**, *100*, 6904-6909. <https://doi.org/10.1021/jp960353d>
- [2] Scheiner, S. Understanding Noncovalent Bonds and their Controlling Forces. *J. Chem. Phys.* **2020**, *153*, 140901. <https://doi.org/10.1063/5.0026168>
- [3] Brown, T.; LeMay, H.; Bursten, B.; Murphy, C.; Woodward, P.; Stoltzfus, M. *Chemistry: The Central Science*; Pearson Prentice Hall, 2005.
- [4] Swain, C.G.; Scott, C.B. Quantitative Correlation of Relative Rates. Comparison of Hydroxide Ion with Other Nucleophilic Reagents toward Alkyl Halides, Esters, Epoxides and Acyl Halides. *J. Am. Chem. Soc.* **1953**, *75*, 141-147. <https://doi.org/10.1021/ja01097a041>
- [5] Pearson, R.G.; Sobel, H.; Songstad, J. Nucleophilic Reactivity Constants toward Methyl Iodide and Trans-Dichlorodi (Pyridine) Platinum (II). *J. Am. Chem. Soc.* **1968**, *90*, 319-326. <https://doi.org/10.1021/ja01004a021>
- [6] Gupta, K.; Roy, D.R.; Subramanian, V.; Chattaraj, P.K. Are Strong Brønsted Acids Necessarily Strong Lewis Acids? *J. Mol. Struct.-THEOCHEM* **2007**, *812*, 13-24. <https://doi.org/10.1016/j.theochem.2007.02.013>
- [7] Geerlings, P.; De Proft, F.; Langenaeker, W. Conceptual Density Functional Theory. *Chem. Rev.* **2003**, *103*, 1793-1874. <https://doi.org/10.1021/cr990029p>
- [8] Forgacs, G.; Colonits, M.; Hargitai, I. The Gas-Phase Molecular Structure of 1-Fluorosilatrane from Electron Diffraction. *Struct. Chem.* **1990**, *1*, 245-250. <https://doi.org/10.1007/BF00674268>
- [9] Rad, A.S.; Shadravan, A.; Soleymani, A.A.; Motaghedi, N. Lewis Acid-Base Surface Interaction of Some Boron Compounds with N-Doped Graphene; First Principles Study. *Curr. Appl. Phys.* **2015**, *15*, 1271-1277. <https://doi.org/10.1016/j.cap.2015.07.018>
- [10] Aichi, M.; Hafied, M.; Dibi, A. Theoretical Study of Pentavalent Halosilicates: Structure and Charge Delocalization. *J. Struct. Chem.* **2021**, *62*, 824-834. <https://doi.org/10.1134/S0022476621060020>
- [11] Adams, R.D.; Captain, B.; Fu W.; Smith, M.D. Lewis Acid-Base Interactions between Metal Atoms and Their Applications for the Synthesis of Bimetallic Cluster Complexes. *J. Am. Chem. Soc.* **2002**, *124*, 5628-5629. <https://doi.org/10.1021/ja017486j>
- [12] Jensen, W. *The Lewis Acid-Base Concepts: An Overview*; John Wiley Sons: New York, 1982.
- [13] Poleshchuk, O.K.; Branchadell, V.; Fateev, A.V.; Legon, A.C. SO_3 Complexes with Nitrogen Containing Ligands as the Object of Nuclear Quadrupole Interactions and Density Functional Theory Calculations. *J. Mol. Struct.-THEOCHEM* **2006**, *761*, 195-201. <https://doi.org/10.1016/j.theochem.2005.12.032>
- [14] Poleshchuk, O.K.; Branchadell, V.; Brycki, B. HFI and DFT Study of the Bonding in Complexes of Halogen and Interhalogen Diatomics with Lewis Base. *J. Mol. Struct.-THEOCHEM* **2006**, *760*, 175-182. <https://doi.org/10.1016/j.theochem.2005.10.016>
- [15] Wiśniewski, M.; Gauden, Pearson's, P.A. Hard-Soft Acid-Base Principle as a Means of Interpreting the Reactivity of Carbon Materials. *Adsorpt. Sci. Technol.* **2006**, *24*, 389-402. <https://doi.org/10.1260/026361706779849744>
- [16] Fukui, K.; Yonezawa, T.; Shingu, H. A Molecular Orbital Theory of Reactivity in Aromatic Hydrocarbons. *J. Chem. Phys.* **1952**, *20*, 722. <https://doi.org/10.1063/1.1700523>
- [17] Parr, R.G.; Szentpaly, L.V.; Liu, S. Electrophilicity Index. *J. Am. Chem. Soc.* **1999**, *121*, 1922-1924. <https://doi.org/10.1021/ja983494x>
- [18] Parr, R.G.; Pearson, R.G. Absolute Hardness: Companion Parameter to Absolute Electronegativity. *J. Am. Chem. Soc.* **1983**, *105*, 7512-7516. <https://doi.org/10.1021/ja00364a005>
- [19] Senet, P. Chemical Hardnesses of Atoms and Molecules from Frontier Orbitals. *Chem. Phys. Lett.* **1997**, *275*, 527-532. [https://doi.org/10.1016/S0009-2614\(97\)00799-9](https://doi.org/10.1016/S0009-2614(97)00799-9)
- [20] Gázquez, J. L.; Cedillo, A.; Vela, A. Electrodonating and Electroaccepting Powers. *J. Phys. Chem. A* **2007**, *111*, 1966-1970. <https://doi.org/10.1021/jp065459f>
- [21] Domingo, L.R.; Chamorro, E.; Pérez, P.J. Understanding the Reactivity of Captodative Ethylenes in Polar Cycloaddition Reactions. A Theoretical Study. *J. Org. Chem.* **2008**, *73*, 4615-4624. <https://doi.org/10.1021/jo800572a>
- [22] Lewis, G.N. *Valence and the Structure of Atoms and Molecules, Chemical Catalog Company*. New York, 1923.
- [23] Abboud, J.-L.M.; Alkorta, I.; Dávalos, J.Z.; Gal, J.-F.; Herberos, M.; Maria, P.-C.; Mó, O.; Molina, M.T.; Notario, R.; Yáñez, M. The $P_4 \cdots Li^+$ Ion in the Gas Phase: A Planetary System. *J. Am. Chem. Soc.* **2000**, *122*, 4451-4454. <https://doi.org/10.1021/ja993732a>
- [24] Cohen, A.; Mori-Sánchez, P.; Yang, W. Challenges for Density Functional Theory. *Chem. Rev.* **2012**, *112*, 289-320. <https://doi.org/10.1021/cr200107z>
- [25] Frisch, M.J.; Trucks, G.W.; Schlegel, H.B.; Scuseria, G.E.; Robb, M.A.; Cheeseman, J.R.; Scalmani, G.; Barone, V.; Petersson, G.A.; Nakatsuji, H. et al. Gaussian 09: Gaussian Inc, Wallingford CT, 2016.
- [26] Salvatori, T.; Dozzi, G.; Cucinella S. Synthesis of N-(Dimethylamino)propyliminodialanes. *Inorganica Chim. Acta* **1980**, *38*, 263-265. [https://doi.org/10.1016/S0020-1693\(00\)91970-4](https://doi.org/10.1016/S0020-1693(00)91970-4)
- [27] Arnett, E.M.; Quirk, R.P.; Burke, J.J. Weak Bases in Strong Acids. III. Heats of Ionization of Amines in Fluorosulfuric and Sulfuric Acids. New General Basicity Scale. *J. Am. Chem. Soc.* **1970**, *92*, 1260-1266. <https://doi.org/10.1021/ja00708a026>
- [28] Gold, V. Glossary of Terms Used in Physical Organic Chemistry. *Pure Appl. Chem.* **1983**, *55*, 1281-1371. <https://doi.org/10.1351/pac198355081281>
- [29] Gal, J.F.; Maria, P.C.; Raczynska, E.D. Thermochemical Aspects of Proton Transfer in the Gas Phase. *J. Mass Spectrom.* **2001**, *36*, 699-716. <https://doi.org/10.1002/jms.202>
- [30] Padmaja, L.; Ravikumar, C.; Sajan, D. Density Functional Study on the Structural Conformations and Intramolecular Charge Transfer from the Vibrational Spectra of the Anticancer Drug Combretastatin-A2. *J. Raman Spectroscopy* **2009**, *40*, 419-428. <https://doi.org/10.1002/jrs.2145>

[31] Depmeier, W.; Schmid, H.; Setter, N.; Werk, M.L. Structure of cubic Aluminate Sodalite, $\text{Sr}_8[\text{Al}_{12}\text{O}_{24}](\text{CrO}_4)_2$. *Acta Cryst.* **1987**, *C43*, 2251-2255 <https://doi.org/10.1107/S0108270187088188>

[32] Fiacco, D.L.; Mo, Y.; Hunt, S.W.; Ott, M.E.; Roberts, A.; Leopold, K.R. Dipole Moments of Partially Bound Lewis Acid-Base Adducts. *J. Phys. Chem A* **2001**, *105*, 484-493. <https://doi.org/10.1021/jp0031810>

[33] Weinhold, F. Natural Bond Orbital Methods. In *Encyclopedia of Computational Chemistry*, vol.3; John Wiley & Sons, Inc.: New York, 1998.

Received: December 21, 2022 / Revised: March 10, 2023 / Accepted: March 23, 2023

ЕФЕКТ ОСНОВНОСТІ ТА НУКЛЕОФІЛЬНОСТІ В ПЕРЕНЕСЕННІ ЗАРЯДУ АДУКТІВ AlH_3 -ОСНОВ: ТЕОРЕТИЧНИЙ ПІДХІД

Анотація. Це дослідження дає змогу вивчити взаємодію кислоти Льюїса (AlH_3) й основ Льюїса: CO ; H_2O ; NH_3 ; PH_3 ; PCl_3 ; H_2S ; CN^- ; OH^- ; O_2^{2-} ; F^- ; $\text{N}(\text{CH}_3)_3$; N_2 ; N_2H_4 ;

N_2H_2 ; $\text{C}_5\text{H}_5\text{N}$; $\text{C}_6\text{H}_5\text{-NH}_2$. За допомогою розрахунків теорії DFT з функціоналом B3LYP з використанням базового набору 6-31G(d,p) і з метою перевірки впливу як донора, так і акцептора на утворення різних адуктів ми зосередилися передусім на розрахунку енергетичної щільності $\Delta E_{\text{ВЗМО-НВМО}}$, енергії Гіббса ΔG , кута (θ) в основі AlH_3 та величини енергії взаємодії E_{inter} . Також розраховували кілька параметрів реакційної здатності (індекс електрофільності (ω), нуклеофільність (N), хімічний потенціал (μ), жорсткість (η) і поляризованість (α)), щоб визначити слабку взаємодію та розрізнити нуклеофільність і основність різних основ Льюїса. Результати показали, що електронне перенесення заряду оцінюється як важливе в системах, де встановлено взаємодію між Al та аніонними основами, а сила донора електронів є передбачуваною для O^{2-} , F^- , OH^- і CN^- . Організація псевдотетраедричних адуктів залежить від геометричних параметрів (довжини зв'язку та кута θ) й енергій Гіббса ΔG , які характеризують головну стабільність.

Ключові слова: кислотно-основна взаємодія Льюїса, стійкість, DFT, аналіз NBO.